Mechanism and Machine Theory 169 (2022) 104645

Contents lists available at ScienceDirect

Mechanism and Machine Theory

journal homepage: www.elsevier.com/locate/mechmt

Research paper

Increasing robustness and output performance of Variable Stiffness Actuators in periodic motions

Trevor Exley, Amir Jafari *

Advanced Robotic Manipulators (ARM) Lab, Department of Biomedical Engineering, University of North Texas, TX, United States

ARTICLE INFO

Keywords:
Variable Stiffness Actuators
Optimization
Robustness

ABSTRACT

Variable Stiffness Actuators (VSAs) have been developed to address the safety and limited adaptability in interactions with uncertainties and energy efficiency issues which exist in traditional "stiff" robots. When desired performance of a VSA is given for a certain application, the question is how this desired performance can be achieved with minimum energy consumption and maximum robustness against uncertainties. This will lead to more compact, lighter but more powerful VSAs. This work develops an understanding of how to optimally design the parameters of the stiffness adjustment mechanisms by developing a framework that can robustly maximize the output performance of VSAs. Five VSA examples, each representing a different design set of stiffness adjustment mechanism, are being considered and evaluated based on the proposed optimization framework to perform a given periodic motion. The resultant optimal design of each set is then compared with the original design in terms of output performance and robustness. The proposed framework shows improvement of the output performance for the given periodic motion up to 546%, with robustness of up to 2.1% perturbation of the optimal design values.

1. Introduction

In contrast to industrial robots that should be operated in isolated work-space from humans, where everything about the environment is already known and planned for, the existence of humans in Human–Robot Interactions (pHRI) applications creates highly unknown environments as we, humans, are so unpredictable when it comes to motion, location, and interaction forces [1]. In order to guarantee safety of humans in physical interactions with robotic manipulators, actuators as the sources of generating mechanical power should behave soft [2]. There are two main approaches to make a robotic platform soft; one, that is called *active compliance* [3–5], is through the control framework, where the actuator should be facilitated with force/torque sensors to detect the collision and close loop feedback with different control strategies to prevent or at least reduce the level of risk [6]. This approach, however, cannot guarantee the safety in case of high bandwidth collisions such as impact forces and, as a result, the actuator would behave rigid in such scenarios. The other approach is to realize *passive compliance* embedded into the mechanical structure of the actuator, so that it can behave inherently soft in any interaction scenario [7–11]. A pioneer in this area, is the *Series Elastic Actuator* SEA developed by G. Pratt [12], where a spring is located between the motor and the output link, decoupling the high reflected inertia of the gearbox from that of the link. Therefore, when it comes to an interaction with a human body, only the link inertia will be in contact. Also, the spring can act like a force sensor, allowing to use the active compliance approach to regulate the reflected stiffness through the control framework on top of the mechanical stiffness [13,14]. But again when it comes to high bandwidth interaction scenarios, the stiffness of a SEA would be the fixed stiffness level of its embedded spring [15].

* Correspondence to: 1155 Union Circle #310440 Dallas-Fort worth Area, TX 76203-5017, United States.
E-mail address: amir.jafari@unt.edu (A. Jafari).

https://doi.org/10.1016/j.mechmachtheory.2021.104645
Received 14 June 2021; Received in revised form 22 September 2021; Accepted 5 November 2021
Available online 9 December 2021

Also note that, spring can save and release the energy, which in periodic motions can greatly enhance the energy efficiency [16, 17]. However, in case of a SEA, this would be beneficial only when the frequency of the desired periodic motion matches the natural frequency of the compliant actuator [18]. In order to exploit the full advantage of having a source of storing and releasing energy, i.e. spring, in periodic motions with different frequencies, the mechanical stiffness level of the actuator should be adjustable [19,20]. Furthermore, In general, when a robotic manipulator moves fast, it should be soft to guarantee safety and when it moves slow and accuracy is desired, it should be rigid [21].

Variable Stiffness Actuators (VSAs) [22–25], have been developed to address these needs in pHRI applications. A VSA needs two motors as it has to control two degrees of freedom; one is the output link's position just like a normal rigid actuator and the other one is the output link's stiffness [26–28]. Regulating the stiffness in VSAs is done by different Stiffness Adjustment Mechanisms (SAMs) that contain springs and other components [29]. SAMs can be categorized into two design groups; *Antagonistic* and *Series* [30]. In antagonistic designs, both motors are responsible to control the output link position and regulating its stiffness, whereas in series designs, one motor is dedicated to the link positioning while the other one adjusts the stiffness.

Despite the great need of being able to regulate the stiffness of the robotic actuators in pHRI applications and tremendous number of different VSAs that have been developed so far, to our knowledge, there is not a VSA that has successfully passed the research lab phase and transitioned into a real application. The main reason is due to the lack of understating how to optimally design a SAM based on desired performances of different applications. If not optimally designed, the additional complexities that SAMs present to the actuators prevent to win the trade-off between benefits of having a SAM versus its costs. Some examples of these trade-off criteria are as following: the energy saving benefit of adjusting the stiffness in different periodic motions compared to how much energy is in fact required for the stiffness regulation, increased torque capacity due to having two motors compared to how much torque can be actually transferred to the output link, energy storage capacity of the springs compared to how much energy can be actually released at the output link side, and adjusting the stiffness to a certain value compared to what is the actual stiffness of the output link in dealing with unknown external forces. Currently, these trade-off criteria are not in favor of introducing a SAM into the actuator. Therefore, generally, having a simple series elastic actuator with active compliance has been preferred over having a complex VSA [31,32]. This research seeks to understand how to optimally design the parameters of a SAM by developing a framework that can robustly maximize the output performance of VSAs to perform a variety of tasks, including periodic motions.

Depending on a particular design, the design parameters of a SAM may include the dimensions of its principal components, e.g. cam, level arm, pulleys, etc, and stiffness of its springs. The constraints are user defined torque and velocity limitations of the motors, springs' constants (stiffnesses), and size limitations of the principal components.

The dimensions of principal components are real continuous variables, while stiffness of the spring and their dimensions, e.g. diameter, length, and maximum allowable deflections, are categorical variables as springs are commercial products that come in different but discrete sizes and stiffness constants. The same holds true for motors and theirs maximum torques and velocities. Furthermore, since power is a product of torque and velocity, the nature of any energy-based optimization problem would be nonlinear. Therefore, we will be dealing with a mixed-integer nonlinear optimization problem with a large number of feasible solutions [33]. To solve this type of optimization problem, there are basically two main approaches; *Heuristic* (or Meta-Heuristic) [34] and *Global optimal* [35]. The heuristic approaches can quickly find optimal solutions but cannot guarantee that the yield solutions are the global optimum (as they may get trapped into local optimal solutions). Examples are: Tabu search [36], Simulated annealing [37], and Ant colony optimization [38]. The global optimal approaches, on the other side, may take a long time to find a solution, but once it is found, the solution is guaranteed to be the global optimal. Since computation time is not a critical factor in optimal design problems, therefore global optimal approach is preferred over the heuristic one. Examples are: Cutting plane method [39], Branch and Bound (BB) algorithm [40] and Interval method [41].

For this optimal design problem, we propose to employ interval method as a mean to systematically enumerate candidate solutions in a BB algorithm. The so called interval based branch and bound algorithm can deal with nonlinear mixed-integer problems and has been shown to be effective in optimal actuator design problems, in particular [42,43].

This article is organized as follow: in Section 2, different sets of stiffness adjustment mechanism are introduced. Section 3, explains the proposed problem formulation, while Section 4 elaborates on the optimization algorithm. Section 5 presents the results obtained from the optimization framework and compares them with the original designs. Finally Section 6 presents conclusion and future works.

2. Stiffness adjustment mechanisms — design sets and principal dimensions

VSAs have been developed to address the safety, limited adaptability in interaction with uncertainties and energy efficiency issues which exist in traditional ''stiff'' robots. These types of actuators have two motors to regulate the stiffness and the position of the attached link. Springs are embedded into the system to realize the variable stiffness functionality using different design principles. In general, these designs can be divided into two main classes: antagonistic and series [44,45] (Fig. 1).

In antagonistic designs, two motors M_1 and M_2 are antagonistically actuating a link through nonlinear springs (i.e. nonlinear force to deflection profile) that are placed between the motors and the link. The nonlinearity of the springs is an important factor as stiffness regulation cannot be achieved using linear springs in these setups. Based on different arrangements of the motors and springs, these types of designs can be realized in three different sub-classes: simple unidirectional (e.g. [46]), cross coupling (e.g. [22]) and bidirectional (e.g. [47]) configurations as it is shown in Fig. 1-a-b-c.

Alternatively, in the series design approaches, one motor M_1 with a spring in series is dedicated to the link positioning while another motor M_2 (usually smaller than M_1) is set to change the stiffness. In one class of these design approaches (Fig. 1-d), nonlinear

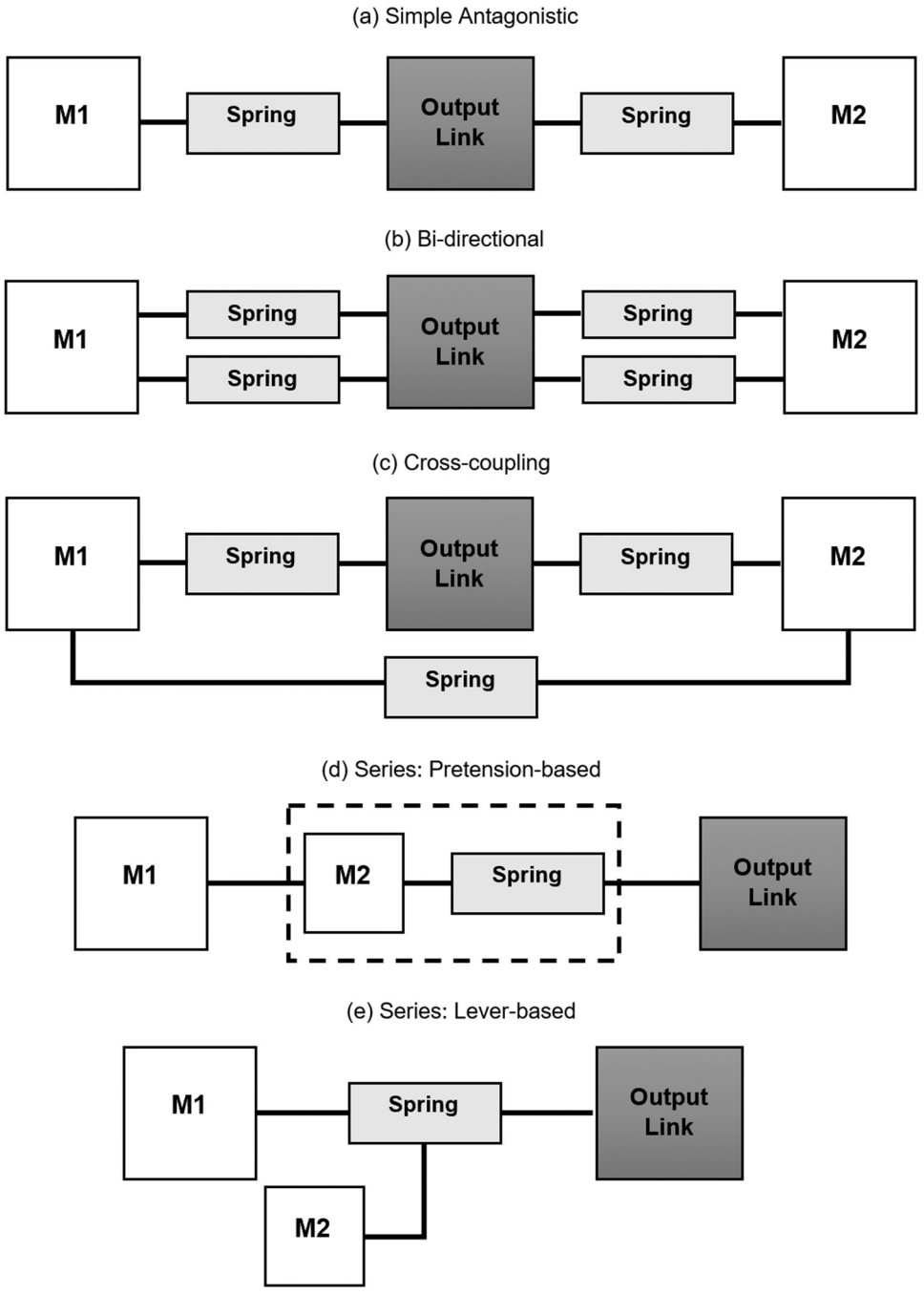

Fig. 1. Different classes of SAMs: Antagonistic Class: (a) simple antagonistic, (b) cross-coupling, (c) bi-directional- Series Class: (d) pre-tension based, and (e) lever-based.

springs are employed where stiffness adjustment is done through changing the pre-tension of the springs using M_2. Another class of these design approaches (lever-based) (Fig. 1-e) uses linear springs while the stiffness adjustment is done through changing another parameter such as location of the springs [27], the pivot point [25,48] or the point at which force is being applied to a lever mechanism [49].

These design approaches can be realized in many different ways, using different mechanisms or components. However, regardless of how they have been realized, there are always principal components in each class whose dimensions or properties are essential in determining functionality of the SAM as well as output performance of the VSA. In antagonistic SAMs, examples are: the radius

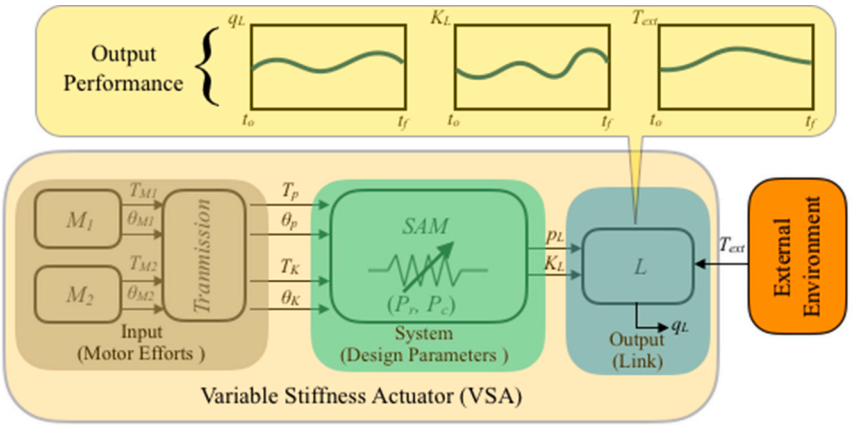

Fig. 2. Schematic of a Variable Stiffness Actuator VSA.

of the link's pulley, the radius of each motor's pulley, the distances between center of rotation of each pulley as well as springs' constants.

In those SAMs that need nonlinear springs, sometimes linear springs are used together with a mechanism that can generate nonlinear force to deflection profile, such as cam-follower mechanism in contact with a spring [50]. In this case, dimension of cam is also another principal component of the SAM as its profile determines the nonlinearity of the spring.

In our proposed optimal design process, we only take into account the principal components of a SAM, rather than every single elements (such as bearings, screws, etc.) that are being used in a particular realization. However, our proposed approach is general and one can consider different detailing levels of a particular SAM in the optimization process. However, it may substantially add to the complexity of the process by increasing the number of variables while the output optimal result might not be significantly better.

In addition, each motor M_1 and M_2 provides energy to the SAM that can be presented by considering torques and displacement/velocity of an element due to that torque (e.g. motor shaft). Motors come in different torque and velocity capacities. These parameters which eventually affect the output performance of a VSA are discrete categorical variables. The same holds true for springs as they have different spring constants, sizes, free length, and maximum allowable deflections, which all can affect the performance of a VSA.

Therefore, in order to optimize the design process, different types of variables including continuous and integer or categorical variables have to be dealt with. This makes the design problem a nonlinear mixed-integer optimization problem.

3. Output performance formulation

If a certain output performance for a VSA is desired in terms of trajectory of the output link, its stiffness profile and an external torque that has to be overcome during a given period of time, then the energy required to achieve this output performance, i.e. output energy can be calculated and compared to the energy that the VSA consumes to perform the task, i.e. input energy (Fig. 2).

This article proposes an optimization framework that can robustly minimizes the VSA's input energy requirement as a function of SAM's design parameters. The significance of this work is that, by optimally designing robust VSAs, the robotic manipulators would be more efficient, more compact, lighter, safer to interact with humans, while at the same time can achieve higher level of performances.

The output energy of a VSA can be determined by the output link's trajectory (velocity and acceleration can be simply calculated by taking first and second derivatives with respect to the time), stiffness as well as the external torque it has to handle during its motion. This energy is indeed provided by the motors as the input energy to the VSA system.

3.1. Performance formulation

Every class of VSA, regardless of being series or antagonistic, can be represented by the schematic shown in Fig. 2. Motors M_1 and M_2 provide torques T_{M_1} and T_{M_2} as well as displacements θ_{M_1} and θ_{M_2} to a transmission system (e.g. gearbox). The transmission system outputs the torque and displacement to change the output link's position T_p and θ_p, as well as the torque and displacement required to adjust the output link's stiffness T_K and θ_K. It should be mentioned here that in ideal series design, simply $T_{M_1} = T_p$, $T_{M_2} = T_K$, $\theta_{M_1} = \theta_p$ and $\theta_{M_2} = \theta_K$. However in antagonistic design these relationships are more complicated and depends on the design parameters. We focus on optimizing the performance of SAM, therefore we assume that the transmission is ideal, i.e. the input energy to the transmission is equal to the output energy delivers by the transmission:

$$E_{in} = \sum_{i=1}^{2} \int_{t_o}^{t_f} T_{M_i}.\dot{\theta}_{M_i} dt = \int_{t_o}^{t_f} T_p.\dot{\theta}_p dt + \int_{t_o}^{t_f} T_K.\dot{\theta}_K dt \tag{1}$$

The output of the transmission will be the input to the SAM. The dynamic equations of both link positioning and stiffness adjustment of a SAM, can then be expressed as follow:

$$\begin{cases} T_p = I_p\ddot{\theta}_p + b_p\dot{\theta}_p + \alpha T_{ela} \\ T_K = I_K\ddot{\theta}_K + b_K\dot{\theta}_K + (1-\alpha)T_{ela} \end{cases} \tag{2}$$

where I_p and b_p are inertia and damping coefficient parameters of the SAM, respectively, whose torques have to be overcome for link positioning through applied T_p. Similarly, I_K and b_K are inertia and damping coefficient parameters of the SAM, respectively, whose torques have to be overcome for link stiffness adjustment through applied T_K. α is a parameter that its value can vary between zero and one (therefore a continuous variable) depending on the class of SAM. For instance, in a perfect series class based on lever mechanism, $\alpha = 1$, which implies that stiffness motor does not have to overcome the elastic torque T_{ela} generated due to the spring's deflection [27]. However, generally some part of elastic torque is overcome by the position torque T_p and the rest through the stiffness torque T_K.

All the inertia and damping components I_p, b_p, I_K and b_K as well as α are functions of design parameters, which have to be determined by the designer prior to the optimization process.

Elastic torque is actually the output torque of the SAM that has to cancel the external torque T_{ext} (this includes the inertia and damping torques associated with the output link itself) applied by the external environment, therefore, $T_{ela} = T_{ext}$. Considering the difference between the expected position of the output link, i.e. p_L and its actual position, i.e. q_L due to the external torque as δ_L (where $K_L = dT_{ext}/d\delta_L$), one can express the output energy that SAM delivers to the external environment as:

$$E_{out} = \int_{t_o}^{t_f} T_{ext}.\dot{\delta}_L dt \tag{3}$$

where $\dot{\delta_L} = \dot{q_L} - \dot{p_L}$. We define the objective function as: $f(\vec{P}_c, \vec{P}_r) = (E_{in}/E_{out}) \geq 1$.

3.2. Time discretization

Since in general, the VSA's performance in terms of output link's trajectory, its stiffness and external torque are given as functions of discrete time and not necessarily as analytical functions, Eqs. (1)–(3) have to be discretized with respect to the time. We discretize time from t_o to t_f of the following functions into n points: q_L, p_L, K_L, $T_{ext}(= T_{ela})$, T_p, T_K, θ_p and θ_K. If $\mathbf{X}$ represents each of these function in discrete fashion, therefore, the time derivative of X, i.e. $\dot{\mathbf{X}}$ (where $\mathbf{X}$ and $\dot{\mathbf{X}} \in \mathbb{R}^n$) can be approximated by $D\mathbf{X} \in \mathbb{R}^{n\times n}$ where:

$$D = \begin{bmatrix} -1 & 1 & 0 & 0 & \dots & 0 \\ 0 & -1 & 1 & 0 & \dots & 0 \\ \vdots & \vdots & \vdots & \vdots & \dots & \vdots \\ 0 & \dots & \dots & \dots & -1 & 1 \end{bmatrix} [1/2\Delta T] \tag{4}$$

and ΔT is the sampling rate, based on the central difference method [51]. With this discretization method, the dynamic equations of a VSA (Eq. (2)) can be approximated as:

$$\begin{cases} \mathbf{T}_p = (I_p D^2 + b_p D)\boldsymbol{\theta}_p + \alpha \mathbf{T_{ela}} \\ \mathbf{T}_K = (I_K D^2 + b_K)\boldsymbol{\theta}_K + (1-\alpha)\mathbf{T_{ela}} \end{cases} \tag{5}$$

Furthermore, there are two more equations that show relationships between $\mathbf{K}_L$, $\boldsymbol{\theta}_p$, $\boldsymbol{\theta}_K$ and $\mathbf{T}_{ela}$ as follow:

$$\begin{cases} \mathbf{K}_L = \mathbf{K}, \mathbf{K}_i = (\mathbf{T}_{ela_{i+1}} - \mathbf{T}_{ela_i})/(\boldsymbol{\delta}_{L_{i+1}} - \boldsymbol{\delta}_{L_i}), \forall i \in 1, 2, \dots, n \\ \mathbf{K}_{L\,model} = f_K(\boldsymbol{\theta}_p) \end{cases} \tag{6}$$

where $\mathbf{K}_{L\,model}$ is model-based stiffness of the output link as a function of $\boldsymbol{\theta}_p$. Such function f_K can be determined based on the class of SAM and its design parameters. Therefore, based on the chosen design parameters, Eqs. (5) and (6) can be used to solve for four input variables: $\mathbf{T}_p$, $\mathbf{T}_K$, $\boldsymbol{\theta}_p$ and $\boldsymbol{\theta}_K$ using given output variables: $\mathbf{T}_{ext}$, $\boldsymbol{\theta}_L$ and $\mathbf{K}_L$.

Once all variables are determined in their discrete fashions, it is possible to calculate both the input and the output energies as:

$$E_{in} = \sum_{i=1}^{n} [(\mathbf{T}_{p\,i})^T D\boldsymbol{\theta}_{p\,i} + (\mathbf{T}_{K\,i})^T D\boldsymbol{\theta}_{K\,i}]\Delta T \tag{7}$$

$$E_{out} = \sum_{i=1}^{n} [(\mathbf{T}_{ela\,i})^T D\boldsymbol{\delta}_{L\,i}]\Delta T \tag{8}$$

Similarly, all design's and actuators' constraints can be discretized with respect to the time.

As discussed before, to design a SAM, we are dealing with some continuous design variables such as dimensions of its principal elements as well as some categorical variables such as stiffness, free length, diameter and maximum allowable deflection of the springs. We present continuous variables as vector $\vec{P}_r \in: \mathbb{R}^n$ (where n is the number of continuous variables) and categorical variables as $\vec{P}_c \in \prod_{i=1}^{c_n} K_i$ (where c_n is the number of categorical variables). Therefore, the optimization problem can be expressed as:

$$\begin{cases} \underset{\vec{P}_c \in \mathbb{R}^n, \vec{P}_c \in \prod_{i=1}^{c_n} K_i}{\text{minimize}} \quad f(\vec{P}_c, \vec{P}_r) = E_{in}/E_{out} \\ \text{subject to:} \\ g_i(\vec{P}_c, \vec{P}_r) \leq 0, \forall i \in 1, \dots, l \\ h_j(\vec{P}_c, \vec{P}_r) = 0, \forall j \in 1, \dots, m \end{cases} \tag{9}$$

This mixed-integer optimization problem is in fact an inverse design problem as oppose to a direct design problem. However, problems of this type are generally nonlinear, nonquadratic, and also nonconvex. Generally, for these problems, the knowledge of all the expressions of the functions of the considered problem can be found through the principal components and their interactions based on what class of VSAs designs the SAM belongs to. However, the solution could not be found by iterating some resolution of the direct problem as there are large number of feasible solutions.

3.3. Robustness formulation

In real world, we always have to deal with uncertainties. In the context of the design optimizations of VSAs, these uncertainties could be due to manufacturing of springs or motors, fabrication and machining of principal components such as pulley, lever, cam profiles, etc. These uncertainties will affect both the optimal solution found for both categorical and real continuous variables and consequently inertia, damping and even available motor torques and velocities. These effects change the coefficients in both the cost function as well the constraints in our formulated optimization problem, in other words, the optimization problem will be perturbed as:

$$\begin{cases} \underset{\vec{P}_c\in\mathbb{R}^n,\vec{P}_c\in\prod_{i=1}^{c_n}K_i}{\text{minimize}} \quad z = f(\vec{P}_c,\vec{P}_r)+\Delta f(\vec{P}_c,\vec{P}_r) \\ \text{subject to:} \\ g_i(\vec{P}_c,\vec{P}_r)+\Delta g_i(\vec{P}_c,\vec{P}_r)\le 0, \forall i\in 1,\dots,l \\ h_j(\vec{P}_c,\vec{P}_r)+\Delta h_j(\vec{P}_c,\vec{P}_r)=0, \forall j\in 1,\dots,m \end{cases} \tag{10}$$

It is important to understand the robustness of our optimized solutions to the uncertainties that is: how and to what extend these perturbations may affect the optimal solutions of the aforementioned optimization problems. Generally, two scenarios are possible: 1- the optimality of the current optimal solution, i.e. z^*, will be invalid and 2- the feasibility of the current optimal solution will be violated. In the first scenario, we will have a new optimal solution due to the perturbations that reduces the objective function. Usually we consider a "user defined" threshold value on this reduction, i.e. Δz, that means that if the reduction in the objective function is less than this threshold value, we still consider the current solution z^* as the optimal solution. In the second scenario, we need to calculate the maximum perturbations on each design and system parameters that do not make the current optimal solution to violate any constraint.

In order to examine these effects, we will use sensitivity analysis technique. Sensitivity analysis discusses "how" and "how much" changes in the parameters of an optimization problem modify the optimal objective function value and the point where the optimum is attained [52].

Sensitivity analysis and duality are two connected concepts. In mathematical optimization theory, duality or the duality principle is the principle that optimization problems may be viewed from either of two perspectives, the primal problem or the dual problem. The solution to the dual problem provides a lower bound to the solution of the primal minimization problem [53].

Interestingly, it has been proven that regardless of how complex and nonlinear is the primal problem, the dual problem is always a convex problem, i.e. it is easy to find a lower bound for the optimal solution of the primal problem [54].

Considering the minimizing optimization problems in Eq. (9) as primal problems, we can define a *dual* problem for each one as:

$$\begin{cases} \underset{z}{\text{maximize}} \\ \text{subject to:} \\ (\vec{P}_c,\vec{P}_r)\in\mathbb{R}^n\times\prod_{i=1}^{c_n}K_i \xrightarrow{g_i(\vec{P}_c,\vec{P}_r)\le 0,\forall i\in 1,\dots,l,h_j(\vec{P}_c,\vec{P}_r)=0,\forall j\in 1,\dots,m} f(\vec{P}_c,\vec{P}_r)\ge z \end{cases} \tag{11}$$

where $\mathbb{R}^n\times\prod_{i=1}^{c_n}K_i$ is the feasible set and $g_i(\vec{P}_c,\vec{P}_r)\le 0,\forall i\in 1,\dots,l, h_j(\vec{P}_c,\vec{P}_r)=0,\forall j\in 1,\dots,m$ is called distinguished domain of the feasible set. So the dual seeks the largest z for which $f(\vec{P}_c,\vec{P}_r)\ge z$ can be inferred from the constraint set.[1]

Assume that the optimal solution of Eq. (9) be, ∞ or -∞ when the problem is infeasible or unbounded, respectively. Looking at Eq. (11) it is obvious that the optimal value of the primal is equal to the optimal value of the dual.

If $z^*=f(\vec{P}_c^{\,*},\vec{P}_r^{\,*})$ is the optimal solution to the primal problem, then solving the dual is tantamount to constructing a proof that $f(\vec{P}_c,\vec{P}_r)\ge z^*$ using the constraints as premises. It is important to highlight that if we can prove $f(\vec{P}_c,\vec{P}_r)\ge z^*$, then the same proof shows that $f(\vec{P}_c,\vec{P}_r)-\Delta f(\vec{P}_c,\vec{P}_r)\ge z^*$, for $\Delta f(\vec{P}_c,\vec{P}_r)\ge 0$. This is important as in sensitivity analysis, the question is that what perturbations will or will not reduce the optimal solution below $z^*-\Delta f(\vec{P}_c,\vec{P}_r)$ if the value of $\Delta f(\vec{P}_c,\vec{P}_r)$ is given.

A solution of the dual problem (11) can be recovered from a BB search tree in the following way. At each node of the tree, a *surrogate* inequality is derived that is violated by the bounding criteria in effect of that particular node. The surrogate will be a non-negative linear combination of some of the constraints and possibly the objective function. A falsified clause[2] can then be inferred from the surrogate, and this serves as the basis for sensitivity analysis. [57] presents a detailed explanation of this process.

[1] Let P and Q be two propositions about x; that is, their truth or falsehood is determined by the value of x. If Q is true for any $x\in D$ for which P is true, then P implies Q with respect to a domain D ($P\xrightarrow{D}Q$) [55].

[2] In logic, a clause is an expression formed from a finite collection of literals (atoms or their negations). A clause is true either whenever at least one of the literals that form it is true (a disjunctive clause, the most common use of the term), or when all of the literals that form it are true (a conjunctive clause, a less common use of the term) [56].

The idea is to determine under what conditions the bound $f(\vec{P}_c, \vec{P}_r) - \Delta f(\vec{P}_c, \vec{P}_r) \geq z^*$ remains valid for problem (10). A sufficient condition for its validity is that the dual solution remains a valid proof schema for $f(\vec{P}_c, \vec{P}_r) - \Delta f(\vec{P}_c, \vec{P}_r) \geq z^*$ as follow: *For a given $\Delta f(\vec{P}_c, \vec{P}_r)$, let λ be the vector of multipliers in the dual problem that is used to obtain a surrogate at each node of the BB algorithm, and thus ${\lambda^p}_i$ denotes the vector of multipliers at node p on ith constraint, as defined by [58]. It has been proven by [59] that $f(\vec{P}_c, \vec{P}_r) - \Delta f(\vec{P}_c, \vec{P}_r) \geq z^*$ as long as ${\lambda^p}_i \geq 0$. Similarly, if ${\lambda^p}_0$ denotes the vector of multipliers at node p on the objective function, $f(\vec{P}_c, \vec{P}_r) - \Delta f(\vec{P}_c, \vec{P}_r) \geq z^*$ as long as ${\lambda^p}_0 = 1$.*

Solution of the programming dual, for example, reveals the sensitivity of the optimal value to perturbations in the primal constraints. Duality provides a general approach to sensitivity analysis. In particular, it provides a practical method of sensitivity analysis for mixed integer problems.

Solving the dual problem in a sense explains why the optimal value is the best possible. Sensitivity analysis can be viewed as part of this explanation: It examines the role of each parameter in the proof of optimality. It may reveal, for example, that certain parameter play no role at all and can be dropped, or that other parameters can be altered in certain ways without affecting the proof [58].

3.4. Constraints formulation

The constraints of this optimization problem are due to the limitations on real continuous design variables, torque and velocity of the motors M_1 and M_2 as well as springs' maximum allowable deflections $\delta_{s_{max}}$. Here we just presents some examples for each type of these constraints.

-*Design constraints*: In antagonistic designs, the principal components are basically the pulleys attached to each motor's shaft and the output link, as well as the connections between each pair of pulleys (that can always be modeled as series combinations of rigid and extendable, i.e. springs, elements). The dimensions of interest therefore, are each pulley's radius r_{M_1}, r_{M_2}, r_p as well as the distance between each pair of pulleys d_1, d_2, d_3. The distance between each pair of pulleys can be determined by taking into account the free length and maximum allowable deflection of the spring that should be placed between the two pulleys. For instance, for simple antagonistic class as shown in Fig. 1-a, this means that: $l_{0_1} + \delta_{s_{max_1}} \leq d_1$.

In addition to that, there is another important design consideration for antagonistic VSAs: in order to achieve symmetrical behavior as well as contribution of both motors in moving the output link, springs have to be placed with a pre-tension and that pre-tension has to be half of their maximum allowable deflection, so when one spring becomes fully deflected, the other one will reach its free length. This pre-tension will also affect the maximum output link's deflection $\delta_{L_{max}}$. For instance for the spring #1 in the antagonistic class as shown Fig. 1-b, this means that : $r_P \times \delta_{L_{max}} \leq 0.5\ \delta_{s_{max_1}}$.

In series, pre-tension based class, design variables that can define the profile of the cam are essential. It is important to mention here that the cam is a representative component of this class and it does not mean that all the pre-tension based VSA use a cam mechanism. However, SAM functionality of every pre-tension based VSA can be modeled using a cam profile. It is important to define the cam profile as a function of output link's deflection, i.e. $r_c = f(\delta_L)$. Another design variable in this class that can define the range of stiffness adjustment is the distance between the output of the stiffness motor and the center of rotation of the output link as shown in Fig. 1-d, d_c. This distance should allow for full deflection of the spring at no-load condition: $l_o + r_{c_{at\delta_L=0}} + \delta_{s_{max}} \leq d_c$.

In series class based on lever mechanism, length of the lever d_l is an important variable to achieve a desired range for stiffness. Also in both series classes, i.e. the pre-tension based and the lever based, a transmission system TS (e.g. a ball screw mechanism) is required to convert rotary motion of the stiffness motor M_2 into a linear motion. The conversion factor can be denoted by variable set N_{TS} that includes all variables that are required to define the torque/force and rotary/linear motion relationships.

-*Actuator constraints*: In majority of the current VSAs, motors M_1 and M_2 are usually electric DC motors. In these motors, the available torque is limited by the Stall torques T_{s_1} and T_{s_1} and the maximum velocity is ω_{max_1} and ω_{max_2}: $\dot{\theta}_{M_i} \leq \omega_{max_i}$ and $T_{M_i} \leq T_{s_i}\ \forall i \in 1, 2$.

Furthermore, in these types of electric DC motors the available torque is a function of velocity: which is the faster the motor runs the less torque it can apply: $T_{M_i} = T_{s_i} \times (1 + \dot{\theta}_{M_i}/\omega_{max_i})\ \forall i \in 1, 2$.

It is important to mention that motor M_1 and M_2 are commercially available products and thus T_{M_1}, T_{M_2}, ω_{max_1} and ω_{max_2} are related to categorical variables as they come in different discrete values, depending on their types, sizes and manufacturers.

-*Spring constraints*: Springs are also commercially available products that come in different types and sizes and thus their stiffnesses (spring's constants) k_s, free lengths l_o, and maximum allowable deflections $\delta_{s_{max}}$ are categorical variables. Actual length of the spring at any time cannot be less/more that its free length when the spring is extension/compression type and also their amount of deflection at any time should be less than or equal to their maximum allowable deflection. In case of extension springs, for example: $l_s \geq l_o$ and $\delta_s \leq \delta_{s_{max}}$.

It is also important to highlight here that commercially available springs are either extension or compression type, and therefore, in our models we do not assume a spring that can be both extended or compressed.

Another important feature of the springs that can be considered here is related to their free length. Sometimes springs have some level of pre-tension already built in their structure. This means that there is a threshold force level that needs to be overcome in order for the spring to start deflecting. This amount of force threshold affect the effective free length of the spring that is different that its actual free length. The actual free length is the length of the spring when there is no force acting on it, while the effective free length is by taking into account how much the force threshold could deflect the spring in the opposite direction and then subtract that amount from the actual free length of the spring.

4. Optimization algorithm

In order to find the global optimal solution to the problems (9), and (10), we propose to use interval based BB algorithm, as it is guaranteed that the global solution will be precisely enclosed at the end of the algorithm.

Interval-based methods have gained considerable interest over the last decade. Two main features distinguish interval-based methods from other methods: they account for uncertainties in the parameter values and computation errors over the floating-point numbers, and they are able to treat the complete search space, thus offering proofs of infeasibility and/or certification of solutions. Because of these features, these methods are being used in several research areas, including robotics, localization, model qualification, and the design of control systems. For example, robots and vehicles can obtain useful information from a set of sensors (e.g., odometers, GPS or gyrocompass). Then, this information is transformed into a set of non-linear systems of constraints. Solving these systems means finding the position, displacement, or required movement for the vehicle/robot. Uncertainties of sensor measurement errors, mechanical parts or floating-point number computation errors are considered by interval-based methods. Interval-based techniques have also been used successfully for localizing nodes in mobile networks and tracking acoustical sources. In designing robust control systems, the quantitative feedback theory method has been studied by interval-based techniques where the feedback of measurable plant/machinery outputs to generate an acceptable response. Usually, the general problem is related to how to design the feedback controller and prefilter such that the desired specifications are satisfied in the region of uncertainty. Interval Branch and Bound strategies are primarily used to solve continuous constraint systems and to handle constrained global optimization problems. These strategies are mathematically rigorous, i.e., they account for the rounding errors that are implied by floating point operations in their implementations.

The principle of this algorithms is based on subdivisions of the considered initial domain into smaller and smaller parts such that one can determine, using interval analysis [60], which box can be discarded. This is because interval computations will produce the proof that a box cannot contain the global solution or prove the fact that at least one constraint could not be satisfied in a box. Therefore, at the end of the algorithm, the global optimum will be enclosed with a given accuracy, however the algorithms must be capable to deal with both real continuous and categorical variables.

The initial pre-step of the proposed optimization process is normalizing the principal components' values. By dividing the actual values of each component to its original value (i.e. the original non-optimal design), a dimensionless value will be obtained (similar process has been adopted in [61]). This has an effect on simplification of the computations and minimizing the effect of rounding errors as mentioned above. At the end of the optimization process, each dimensionless parameter is then converted to its final optimal value by multiplying the dimensionless and the original non-optimal. The final result will be a dimension-ed value.

The main idea is to subdivide the initial domain space $X \subseteq \mathbb{R}^n \times \prod_{i=1}^{c_n} K_i$ into smaller sub-boxes $Z \subseteq X$ and to delete the considered box Z, if and only if it can be proven that Z cannot contain the global optimum.

In order to subdivide the domain into smaller boxes, we need to consider the space in which the boxes are located in. In this problem, this space is a combination of continuous as well as categorical variables.

BB algorithms have been modified to deal with integer variables, such as in the author's previous work in finding an optimal solution to the facility layout problem [62]. The categorical variables cannot be directly considered in subdivision of a box and an expression of a function. In this project, we propose a method to change categorical variables into integer ones. This is done through an univariate function a that assigns an integer to a categorical value. For example, if one spring has stiffness of 315 N/mm and stiffness of another spring is 450.5 N/mm, this univariate function assigns integer value = 1 to the first stiffness value and integer value = 2 to the second one: $a(1) = 315$ N/mm and $a(2) = 450.5$ N/mm. Therefore, while integer values 1 and 2 can be used for the purpose of subdividing the boxes, the values $a(1)$ and $a(2)$ will be used in calculating the objective function and constraints.

The classical principle of subdividing is to choose a coordinate direction parallel to which Z has an edge of maximum length. Then, Z is subdivided normal to this direction [60]. For continuous variables the subdivision of a box Z on its kth component into to boxes Z_{1k} and Z_{2k} will be applied at the midpoint (as defined in [60]) of the original box Z as follow: $Z_{1k} = [Z_k^L, (Z_k^U + Z_k^L)/2]$ and $Z_{2k} = [(Z_k^U + Z_k^L)/2, Z_k^U]$, where Z_k^L and Z_k^U denote the lower and upper bounds of kth component of box Z, respectively. For categorical variables, however, this subdivision rule has to be slightly modified as follow: $Z_{1k} = [Z_k^L, [(Z_k^U + Z_k^L)/2]_I]$ and $Z_{2k} = [[(Z_k^U + Z_k^L)/2]_I + 1, Z_k^U]$, where $[x]_I$ is the integer part of x.

At each step of the BB algorithm, and as the branches are generated through subdividing the boxes, we will have an interval for each variable. The interval analysis proposed by [60] is a powerful tool to calculate upper and lower bounds of a function over a box. This is simply done by the concept of *natural extension* of a function.

The natural extension of an expression of f into interval consists by replacing each occurrence of a variable by its corresponding interval (which encloses it), and then by applying the rules of interval arithmetic as explained in [60]. For example, if $f(x) = x^2 + x + 1$ and $x \in X = [1, 2]$, then $F(X) = ([1, 2])^2 + [1, 2] + 1$ (X and $F(X)$ are both intervals) is the natural extension of $f(x)$ over box X. It has been proven by [63] that the natural extension is always an inclusion function, which means that it encloses the upper and lower bounds of f over the box (or even all boxes when dealing with multiple variables) X. Therefore, $f(X) = [\min_{x \in X} f(x), \max_{x \in X} f(x)] \subseteq F(X) \forall X$.

Interval arithmetic is only defined for continuous functions, and thus in our method, the inclusion functions must be extended to deal with discrete variables as well. As mentioned before, we will convert categorical variables into integer variables through univariate functions. These integer variables will then be further relaxed into continuous variables. For example, if an integer variable belongs to set $Z^L, Z^L + 1, Z^L + 2, \ldots, Z^U$, a continuous interval $[Z^L, Z^U]$ will be considered for this variable. Replacing an integer set by its corresponding relaxed continuous interval, an inclusion function can then be constructed. The proof is obvious because it comes from the fact that the relaxed compact interval sets enclose by definition the initial discrete sets.

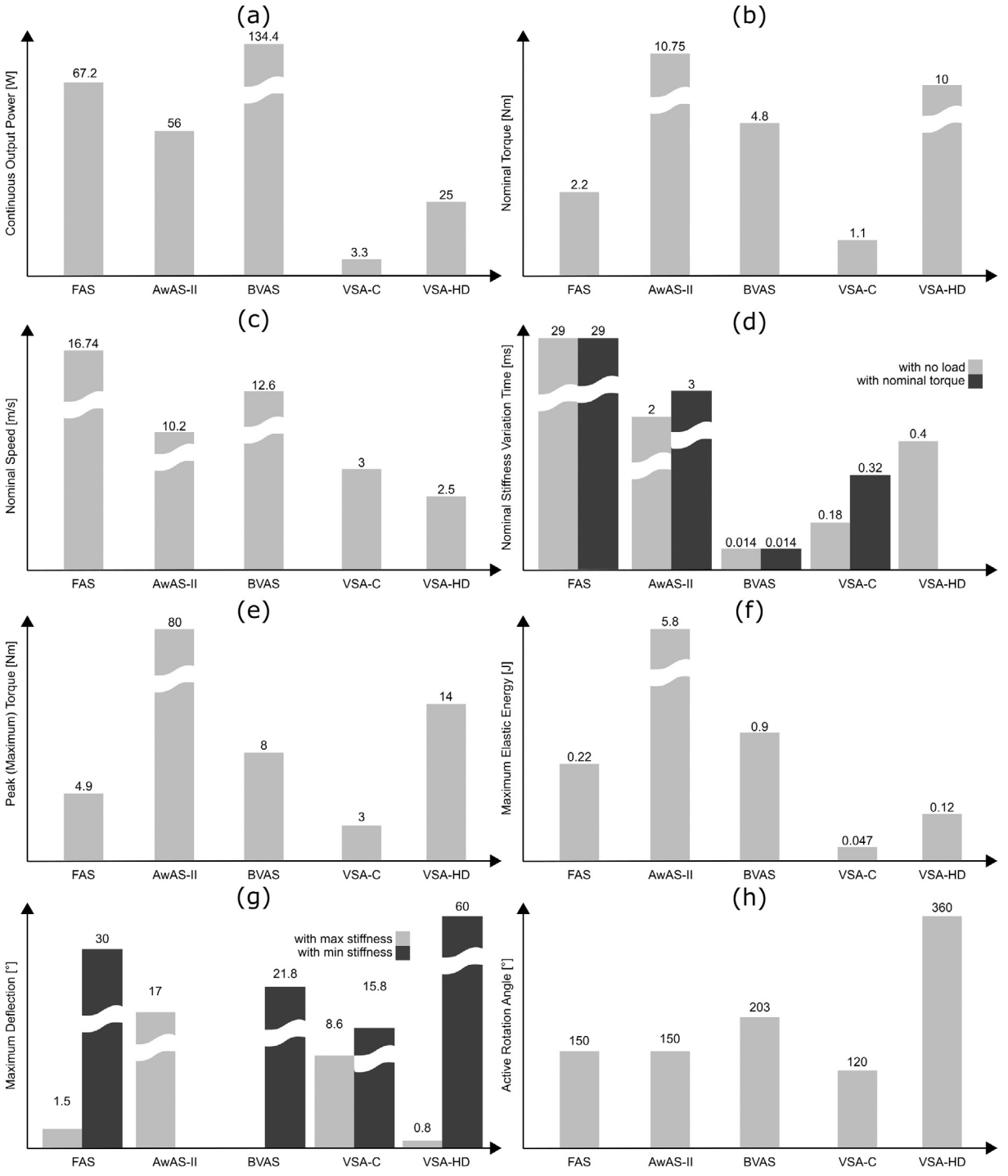

Fig. 3. Plotting actuator constraints for each classes of SAMs: Antagonistic Class: VSA-HD [64] simple antagonistic, VSA-C [65] cross-coupling, and BVAS [47] bi-directional. Series Class: FAS [66] pre-tension based, and AwAS-II [25] lever-based. Constraints include (a) continuous output power, (b) nominal torque, (c) nominal speed, (d) nominal stiffness variation time, (e) peak torque, (f) maximum elastic energy, (g) maximum deflection, and (h) active rotation angle. All data extracted from VIACTORS project's website.

In order to proceed with the elimination of the boxes that cannot contain the global optimum solution, just the computation of lower bound of a given function f over a box Z, i.e. $lb(f, Z)$, is needed. We will compute these bounds by using interval analysis

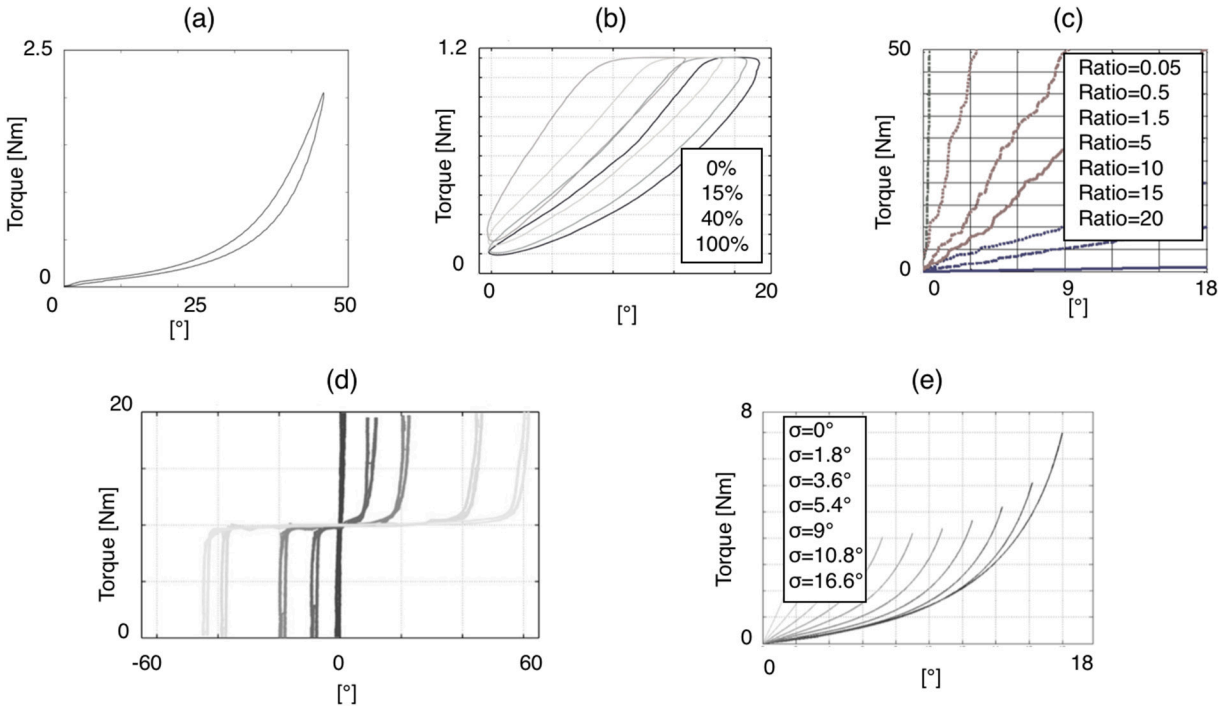

Fig. 4. Plotting static stiffness by applying a known torque and measuring the link deflection for: (a) FSA [66], (b)VSA-C [65], (c) AwAS-II [25], (d) VSA-HD [64] and (e) BVAS [47]. Stiffness is the slop of each curve.

as follow: Considering that $\tilde{f}$ denotes the current solution (in fact, it is just the best evaluation of f at this stage of the algorithm such that all the constraints are satisfied), one obtains the following:

(1) No global solution is in Z, if $ib(f, Z) > \tilde{f}$, a lower bound of f over Z is greater than a solution already found, then no point in Z can be a global minimum.

(2) No feasible solution is in Z, if it exists k such that $ib(g_k, Z) > 0$, or it exists k such that $ib(h_k, Z) > 0$ or $ub(h_k, Z) > 0$ (ub = upper bound). In this case, a very small positive real value can be considered instead of 0, in order to address numerical approximation difficulties due to the floating point operations [60].

This implies that at the end of the algorithm, accurate enclosures of the global minimum value and of all their corresponding solutions can be expected. Indeed, at each step of the algorithm, one has the following properties for all the remaining sub-boxes $Z \subseteq X$: (1) $lb(f, Z) \leq \tilde{f}$ and (2) all constraints are always satisfied.

Algorithm 1 Branch and Bound Algorithm

1: set initial box X := $\mathbb{R}^n \times \prod_{i=1}^{c_n} K_i$
2: set current solution $\tilde{f}$:= + ∞
3: set initial lower bound ℓ := (+∞, X)
4: extract from ℓ the lowest lower bound lb
5: divide the chosen box V by its midpoint m to get sub-boxes V_1 and V_2
6: **for** j=1,2 **do**
   calculate $v_j = lb(f, V_j)$
   calculate lower bounds of all constraints over V_j using interval analysis
   if $\tilde{f} \geq v_j$ and all constraints are satisfied then:
   a: $\ell \leftarrow (v_j, V_j)$
   b: set $\tilde{f}$:= $min[\tilde{f}, f(m_j)]$ if and only if all constraints are satisfied at m_j
   c: if $\tilde{f}$ has been changed from its previous value, then remove all (z,Z) from ℓ where $z > \tilde{f}$
7: **if** $min_{(z,Z)\in\ell} z = \tilde{f}$ STOP, **then**
   else GoTo step 4
8: **end if**
9: **end for**

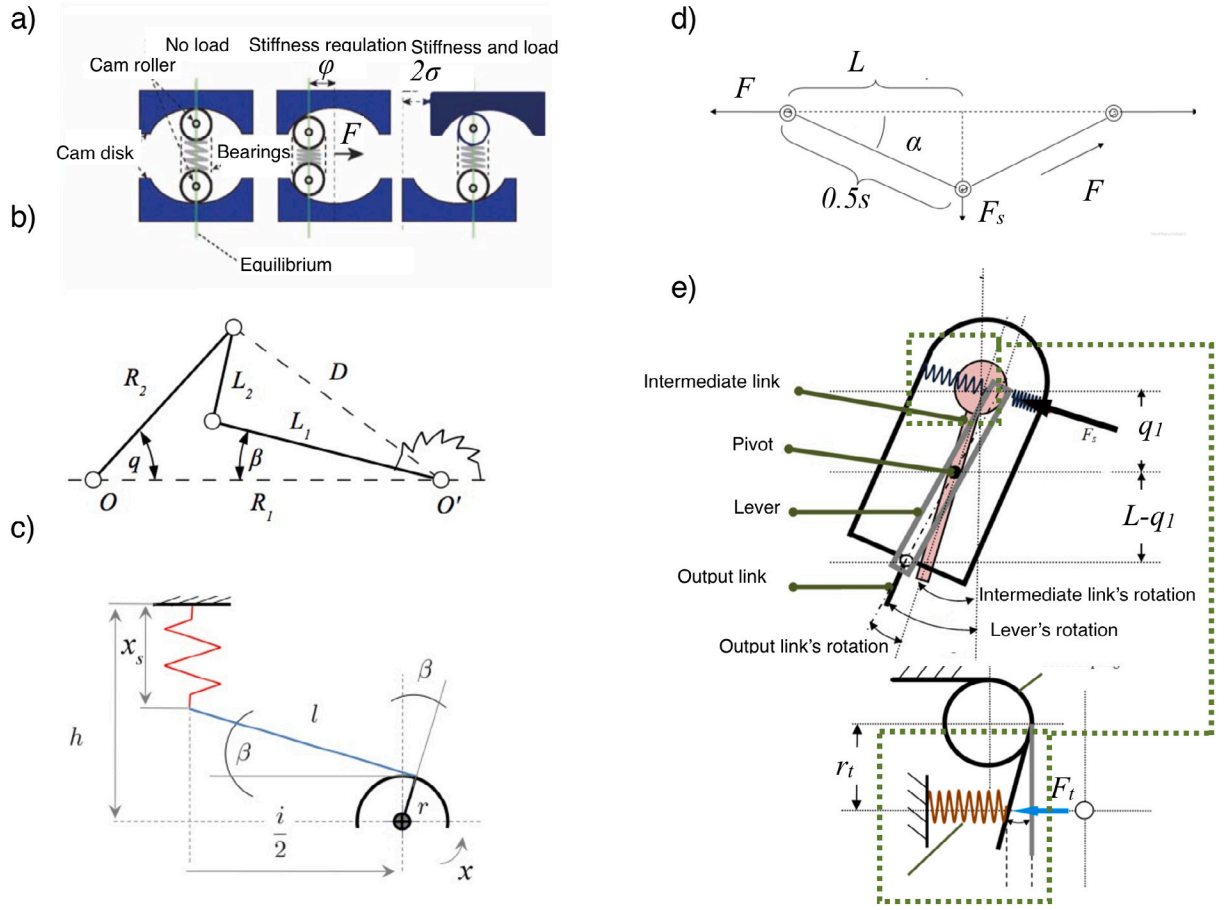

Fig. 5. Schematics of working principles and SAM's principal components of: (a) BVAS [47], (b) VSA-HD [64], (c) VSA-C [65], (d) FAS [66] and (e) AwAS-II AwAS-II [25].

5. Results and discussion

In this section, we provide a comparison analysis on the energy required to perform a specific task done by different VSAs. These intake energy amounts are being calculated theoretically, based on the equations given in Section 3. It is important to mention here that these energy amounts, are in fact, the minimum input energy required to perform the task for each VSA. This is because friction and other fabrication-dependent parameters, such as smoothness of the sliding surfaces, inherent damping of actual springs, etc have not been taken into accounts. These parameters would add to the minimum required energy and thus the actual energy required to perform the task will increase for each VSA. Five Representative examples of SAMs classes, Fig. 1, with their actuators' constraints are being considered as following: Antagonistic Class: VSA-HD [64] simple antagonistic; VSA-C [65] cross-coupling; BVAS [47] bi-directional- Series Class: FSA [66] pre-tension based, and AwAS-II [25] lever-based. Data regarding both actuators and designs constraints for each actuator is extracted from Variable Impedance ACTuation systems embodying advanced interaction behaviORS (VIACTORS) project's website. There are two missing values, first one is regarding the maximum torque hysteresis of AwAS-II, which is being adopted from its previous version AwAS [27] as 21%, and the second one is the nominal stiffness variation in time for VSA-HD with nominal torque, which is being considered to be 0.4 ms as the nominal stiffness variation in time with no load.

The energy equation for each of these five representative actuator example has been provided in VIACTORS's data sheets. These energy equation are functions of joint stiffness, link deflection and other principal dimensions for each actuator. Plugging the provided energy functions into Eqs. (1), (2) and performing the proposed optimization procedure on each actuator, the optimal design parameters for each actuator can be achieved while the design's and actuator's constraints presented in Fig. 3 are all being satisfied.

For each actuator, the torque versus link deflection, Fig. 4 has been obtained experimentally by applying a known weight to the tip of the link at a known distance (hence a known torque) and measuring the resultant angular deflection through a link encoder, while stiffness has been set to different levels in an off-line fashion. The static stiffness can then be calculated by taking derivative of each resultant torque versus deflection curve, to validate the stiffness regulation formulas that have been provided in the actuator's

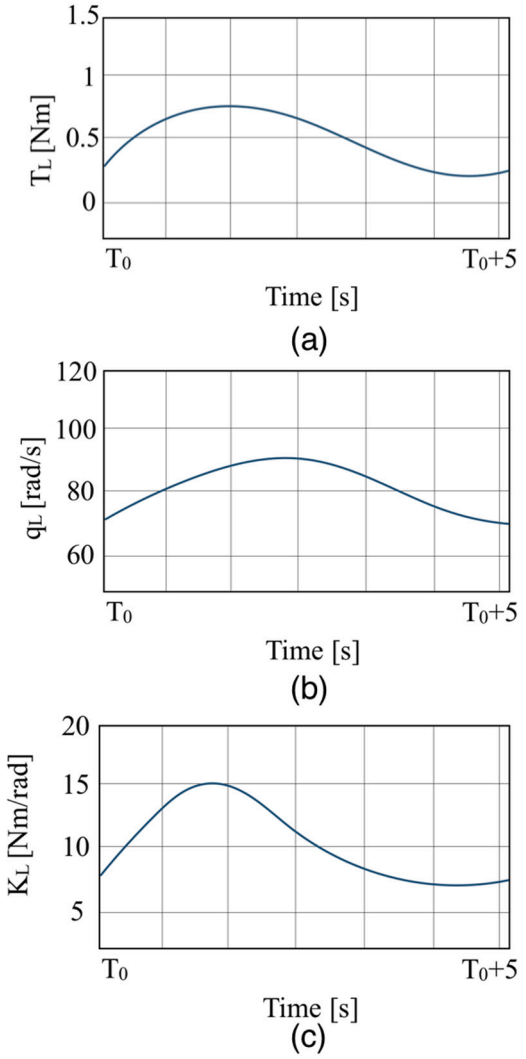

Fig. 6. Desired performance in terms of a periodic motion: (a) desired external load, (b) desired link's trajectory, and (c) desired external link's stiffness.

data sheet in VIACTORS website. The calculated stiffness values are actuators' constraints that have to be satisfied while searching for optimal design parameters using the proposed algorithm.

The principal components of each representative VSA can be extracted from the schematic of their working principles depicted in Fig. 5. In BVAS system, a spring in connected to two cam roller at its ends and is placed between two disks with inner cam profiles as depicted in Fig. 5-a. The distance between the central axis on the two cam profiles and longitudinal axis of the spring, i.e. ϕ, defines the stiffness profile. Deflection of the output link results in deviation of central axis of the upper disk from the fixed lower one by 2δ. In VSA-HD system, a four-bar linkage is connected between motor output, i.e. O' and output link, i.e. O. By applying external torque, the link R_2 will rotate by q, which results in spring's deflection. On the other side, rotating the link L_1 by the co-contraction of the motors, also results in spring's deflection. The stiffness adjustment in CSA-C is done through the mechanism shown in Fig. 5-c: i, the distance between centers of the pulleys; l, distance between free end of the spring and point in which the tendon is tangent to the pulley; r radius of the pulley; β, the angle between i and l; h the distance between fixed end of the spring and i; x the length of the spring and k, the spring elastic constant. FAS is an VSA, where the force F applied through the cable to the output link, indirectly applies a spring force of F_s, at the angle α, through a pulley mechanism with two segmented distances of $0.5S$ each. In AwAS-II actuator, the pivot is at the distance of q_1 from the center of rotation of a lever with the length of L. By applying an output torque, a force of F_t will be applied to the spring's leg at the distance of r_t.

We considered a particular periodic motion as depicted in Fig. 6 in terms of T_L; the link's external load, K_L; the link's stiffness and q_L; the link's trajectory, within a period of 5 s, starting from an arbitrary initial time T_0. All these conditions are considered so that each five representative actuators are able to perform the desired task. The energy required to perform this task was numerically calculated as: 0.23 [J].

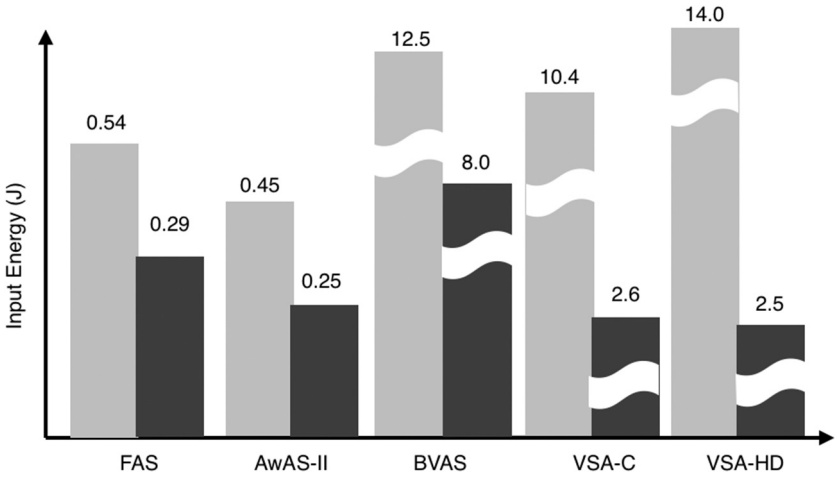

Fig. 7. Input energy required by: FAS [66], AwAS-II [25], BVAS [47], VSA-C [65], VSA-HD [64], to perform the desired task.

Table 1
Examples of principal components with real continuous and/or integer parameters, both original and optimal values as well as maximum allowable perturbation in % by which the resultant values are still optimal.

Actuator	Principal component	Original value	Optimal value	Maximum allowable perturbation %
BVAS	x [m]	0.05	0.005	5.3
BVAS	σ [m]	0.01	0.01028	3.7
BVAS	ϕ [m]	0.015	0.01444	3.5
BVAS	K_s [N/m]	240	320	NA
VSA-HD	R_1 [m]	0.02	0.03247	7.2
VSA-HD	R_2 [m]	0.015	0.012223	2.4
VSA-HD	L_1 [m]	0.01	0.0054	2.1
VSA-HD	L_2 [m]	0.017	0.02545	3.0
VSA-HD	K_s [N/m]	27	27	NA
VSA-cube	h [m]	0.008	0.012404	3.7
VSA-cube	i [m]	0.012	0.012538	5.5
VSA-cube	r [m]	0.004	0.0033	3.6
VSA-cube	K_s [N/m]	2	4	NA
FSA	s [m]	0.014	0.06723	11.3
FSA	L [m]	5	5.329	5.8
FSA	α [°]	25	31.685	4.3
FSA	K_s [N/m]	12	18	NA
AwAS-II	L [m]	0.23	0.12	12
AwAS-II	r_t [m]	0.08	0.02	5.9
AwAS-II	K_s [N/m]	147	220	5.0

The result of the interval-based optimization framework is presented in Fig. 7 and Table 1 for all five representative actuators.

In Fig. 7, the energy required by each VSA to perform the desired task, i.e. the input energy, has been shown for both original and optimal designs. As it is clear, in original FAS the required energy is 0.54 J, while its optimal design requires only 0.29 J, i.e. almost 50% reduction. The same level of energy reduction is being achieved with optimal design of AwAS-II, compared to its original design. Antagonistic designs, generally require lot more energy than series classes. The reason is due to the antagonistic arrangements of motors and springs. In order to regulate the stiffness, motors have to co-contract. Co-contraction is, in fact, two motors "fighting" against each other and "waste" energy. In antagonistic designs, BVAS shows almost 64% energy reduction through optimization process. VSA-C and VSA-HD shows highest required energy to perform the task with their original designs. However, through optimization, the required energy reduce to a great extent, i.e. 7.8 J for VSA-C and 11.5J for VSA-HD. It should be highlighted here, that even with our proposed optimization procedure, the reduction in the required energy in antagonist designs cannot still lead to winning the race against series designs, even if they are not optimally designed. However, this would not weaken the applicability of our proposed optimization process, as the compression should be done between original and optimal designs of each actuator, rather than between each actuators.

In overall, the required input energy for all five VSAs has been dramatically lowered through the proposed optimization process, especially the antagonistic setups, i.e. BVAS, VSA-C and VSA-HD showed more energy reduction where VSA-HD benefited the most by its optimal designs, as much as 546%.

With regards to robustness of the optimal values of the principal components, and as shown in Table 1, the maximum allowable perturbation for each parameter, found to be in the range of 2.1% to 12% of their optimal values obtained as the result of the

proposed optimization algorithm. Sensitivity cannot be defined for discrete parameters such as stiffness values of the springs. It should be mentioned here that the "non-applicability" of the stiffness values should not be generalized to all discrete parameters. For example, if we had the possibility of changing stiffness constants of springs in much smaller intervals that what is available in the market, then springs with different but close stiffness values could all fit within an acceptable range. The most sensitive component found to be L_1 in VSA-HD's four-bar linkage as it is shown in Fig. 5-b (2.1%), while the least sensitive parameter was the length of the lever L in AwAS-II, as shown in Fig. 5-e.

6. Conclusion

This paper presents an interval-based optimization framework to maximize the output performance of variable stiffness actuators, which is defined as the energy required to perform a desired task versus the energy that the VSA actually spend. The desired task is defined as the output link's stiffness, load and trajectory. Even though the proposed approach is applicable to any arbitrary task, here we focus on periodic motions, as in these type of tasks, performing an optimization process is only required for one full period. In addition to that, we also analyzed robustness on the obtained optimal values, in such a way that even with some degree of perturbation, the obtained result still remained optimal. The result showed huge improvements in term of output performance for all classes on stiffness adjustment mechanisms, especially for antagonistic ones up to 546%, while the obtained values were robust to perturbations more than 2.1% of their optimal values. In conclusion, our proposed optimization approach was proved to be very beneficial when designing a VSA to perform a particular desired task which in return can dramatically reduces the energy consumption, size, weight and safety of these VSAs to be used in pHRI applications.

Declaration of competing interest

The authors declare that they have no known competing financial interests or personal relationships that could have appeared to influence the work reported in this paper.

Acknowledgments

This work has been partially supported by the National Science Foundation (NSF), United States award number 2045177.

References

[1] A. Cherubini, R. Passama, A. Crosnier, A. Lasnier, P. Fraisse, Collaborative manufacturing with physical human–robot interaction, Robot. Comput.-Integr. Manuf. 40 (2016) 1–13.
[2] S. Haddadin, E. Croft, Physical human–robot interaction, in: Springer Handbook of Robotics, Springer, 2016, pp. 1835–1874.
[3] B. Davies, S. Harris, W. Lin, R. Hibberd, R. Middleton, J. Cobb, Active compliance in robotic surgery—the use of force control as a dynamic constraint, Proc. Inst. Mech. Eng. H: J. Eng. Med. 211 (4) (1997) 285–292.
[4] C.A. Klein, R.L. Briggs, Use of active compliance in the control of legged vehicles, IEEE Trans. Syst. Man Cybern. 10 (7) (1980) 393–400.
[5] W.S. Kim, A.K. Bejczy, B. Hannaford, Active compliance and damping in telemanipulator control, 1991.
[6] A. De Luca, F. Flacco, Integrated control for phri: Collision avoidance, detection, reaction and collaboration, in: 2012 4th IEEE RAS & EMBS International Conference on Biomedical Robotics and Biomechatronics (BioRob), IEEE, 2012, pp. 288–295.
[7] W. Wang, R.N. Loh, E.Y. Gu, Passive compliance versus active compliance in robot-based automated assembly systems, Ind. Robot: Int. J. 25 (1) (1998) 48–57.
[8] M. Okada, Y. Nakamura, S. Ban, Design of programmable passive compliance shoulder mechanism, in: Proceedings 2001 ICRA. IEEE International Conference on Robotics and Automation (Cat. No. 01CH37164), Vol. 1, IEEE, 2001, pp. 348–353.
[9] D. Chakarov, Study of the passive compliance of parallel manipulators, Mech. Mach. Theory 34 (3) (1999) 373–389.
[10] R.v. Ham, T. Sugar, B. Vanderborght, K. Hollander, D. Lefeber, Compliant actuator designs, IEEE Robot. Autom. Mag. 3 (16) (2009) 81–94.
[11] B. Vanderborght, R. Van Ham, D. Lefeber, T.G. Sugar, K.W. Hollander, Comparison of mechanical design and energy consumption of adaptable, passive-compliant actuators, Int. J. Robot. Res. 28 (1) (2009) 90–103.
[12] G.A. Pratt, M.M. Williamson, Series elastic actuators, in: Proceedings 1995 IEEE/RSJ International Conference on Intelligent Robots and Systems. Human Robot Interaction and Cooperative Robots, Vol. 1, IEEE, 1995, pp. 399–406.
[13] J. Pratt, B. Krupp, C. Morse, Series elastic actuators for high fidelity force control, Ind. Robot: Int. J. 29 (3) (2002) 234–241.
[14] D.W. Robinson, Design and Analysis of Series Elasticity in Closed-Loop Actuator Force Control (Ph.D. thesis), Massachusetts Institute of Technology, 2000.
[15] J. Hurst, A. Rizzi, D. Hobbelen, Series elastic actuation: Potential and pitfalls, in: International Conference on Climbing and Walking Robots, 2004.
[16] N. Paine, S. Oh, L. Sentis, Design and control considerations for high-performance series elastic actuators, IEEE/ASME Trans. Mechatronics 19 (3) (2013) 1080–1091.
[17] S. Stramigioli, G. van Oort, E. Dertien, A concept for a new energy efficient actuator, in: 2008 IEEE/ASME International Conference on Advanced Intelligent Mechatronics, IEEE, 2008, pp. 671–675.
[18] T. Verstraten, P. Beckerle, R. Furnémont, G. Mathijssen, B. Vanderborght, D. Lefeber, Series and parallel elastic actuation: Impact of natural dynamics on power and energy consumption, Mech. Mach. Theory 102 (2016) 232–246.
[19] B. Vanderborght, B. Verrelst, R. Van Ham, M. Van Damme, D. Lefeber, B.M.Y. Duran, P. Beyl, Exploiting natural dynamics to reduce energy consumption by controlling the compliance of soft actuators, Int. J. Robot. Res. 25 (4) (2006) 343–358.
[20] A. Jafari, N.G. Tsagarakis, D.G. Caldwell, Exploiting natural dynamics for energy minimization using an actuator with adjustable stiffness (awas), in: 2011 IEEE International Conference on Robotics and Automation, IEEE, 2011, pp. 4632–4637.
[21] G. Tonietti, R. Schiavi, A. Bicchi, Design and control of a variable stiffness actuator for safe and fast physical human/robot interaction, in: Robotics and Automation, 2005. ICRA 2005. Proceedings of the 2005 IEEE International Conference on, IEEE, 2005, pp. 526–531.
[22] R. Schiavi, G. Grioli, S. Sen, A. Bicchi, Vsa-ii: A novel prototype of variable stiffness actuator for safe and performing robots interacting with humans, in: 2008 IEEE International Conference on Robotics and Automation, IEEE, 2008, pp. 2171–2176.
[23] L.C. Visser, S. Stramigioli, A. Bicchi, Embodying desired behavior in variable stiffness actuators, IFAC Proc. Vol. 44 (1) (2011) 9733–9738.

[24] S. Wolf, G. Grioli, O. Eiberger, W. Friedl, M. Grebenstein, H. Höppner, E. Burdet, D.G. Caldwell, R. Carloni, M.G. Catalano, et al., Variable stiffness actuators: Review on design and components, IEEE/ASME Trans. Mechatronics 21 (5) (2015) 2418–2430.
[25] A. Jafari, N.G. Tsagarakis, D.G. Caldwell, Awas-II: A new actuator with adjustable stiffness based on the novel principle of adaptable pivot point and variable lever ratio, in: Robotics and Automation (ICRA), 2011 IEEE International Conference on, IEEE, 2011, pp. 4638–4643.
[26] A. Jafari, N.G. Tsagarakis, B. Vanderborght, D.G. Caldwell, A novel actuator with adjustable stiffness (AwAS), in: 2010 IEEE/RSJ International Conference on Intelligent Robots and Systems, IEEE, 2010, pp. 4201–4206.
[27] A. Jafari, N.G. Tsagarakis, D.G. Caldwell, A novel intrinsically energy efficient actuator with adjustable stiffness (AwAS), IEEE/ASME Trans. Mechatronics 18 (1) (2011) 355–365.
[28] A. Jafari, N. Tsagarakis, D. Caldwell, Energy efficient actuators with adjustable stiffness: a review on awas, awas-II and compact VSA changing stiffness based on lever mechanism, Ind. Robot: Int. J. 42 (3) (2015) 242–251.
[29] A. Jafari, Coupling between the output force and stiffness in different variable stiffness actuators, in: Actuators, Vol. 3, Multidisciplinary Digital Publishing Institute, 2014, pp. 270–284.
[30] A. Jafari, N.G. Tsagarakis, I. Sardellitti, D.G. Caldwell, How design can affect the energy required to regulate the stiffness in variable stiffness actuators, in: 2012 IEEE International Conference on Robotics and Automation, IEEE, 2012, pp. 2792–2797.
[31] M. Grimmer, A. Seyfarth, Stiffness adjustment of a series elastic actuator in an ankle-foot prosthesis for walking and running: The trade-off between energy and peak power optimization, in: 2011 IEEE International Conference on Robotics and Automation, IEEE, 2011, pp. 1439–1444.
[32] M. Grimmer, M. Eslamy, S. Gliech, A. Seyfarth, A comparison of parallel-and series elastic elements in an actuator for mimicking human ankle joint in walking and running, in: 2012 IEEE International Conference on Robotics and Automation, IEEE, 2012, pp. 2463–2470.
[33] C.A. Floudas, Nonlinear and Mixed-Integer Optimization: Fundamentals and Applications, Oxford University Press, 1995.
[34] K.Y. Lee, M.A. El-Sharkawi, Modern Heuristic Optimization Techniques: Theory and Applications to Power Systems, Vol. 39, John Wiley & Sons, 2008.
[35] R. Horst, P.M. Pardalos, Handbook of Global Optimization, Vol. 2, Springer Science & Business Media, 2013.
[36] F. Glover, M. Laguna, Tabu search, in: Handbook of Combinatorial Optimization, Springer, 1998, pp. 2093–2229.
[37] P.J. Van Laarhoven, E.H. Aarts, Simulated annealing, in: Simulated Annealing: Theory and Applications, Springer, 1987, pp. 7–15.
[38] M. Dorigo, G. Di Caro, Ant colony optimization: a new meta-heuristic, in: Proceedings of the 1999 Congress on Evolutionary Computation-CEC99 (Cat. No. 99TH8406), Vol. 2, IEEE, 1999, pp. 1470–1477.
[39] M. Grötschel, Y. Wakabayashi, A cutting plane algorithm for a clustering problem, Math. Program. 45 (1–3) (1989) 59–96.
[40] E.L. Lawler, D.E. Wood, Branch-and-bound methods: A survey, Oper. Res. 14 (4) (1966) 699–719.
[41] E.R. Hansen, Global optimization using interval analysis: the one-dimensional case, J. Optim. Theory Appl. 29 (3) (1979) 331–344.
[42] F. Messine, V. Monturet, B. Nogarède, An Interval Branch and Bound Method Dedicated to the Optimal Design of Piezoelectric Actuators, Citeseer, 2001.
[43] F. Messine, B. Nogarede, J.-L. Lagouanelle, Optimal design of electromechanical actuators: a new method based on global optimization, IEEE Trans. Magn. 34 (1) (1998) 299–308.
[44] B. Vanderborght, A. Albu-Schäffer, A. Bicchi, E. Burdet, D.G. Caldwell, R. Carloni, M. Catalano, O. Eiberger, W. Friedl, G. Ganesh, et al., Variable impedance actuators: A review, Robot. Auton. Syst. 61 (12) (2013) 1601–1614.
[45] B. Vanderborght, A. Albu-Schäffer, A. Bicchi, E. Burdet, D. Caldwell, R. Carloni, M. Catalano, G. Ganesh, M. Garabini, M. Grebenstein, et al., Variable impedance actuators: Moving the robots of tomorrow, in: 2012 IEEE/RSJ International Conference on Intelligent Robots and Systems, IEEE, 2012, pp. 5454–5455.
[46] T. Ménard, G. Grioli, A. Bicchi, A stiffness estimator for agonistic–antagonistic variable-stiffness-actuator devices, IEEE Trans. Robot. 30 (5) (2014) 1269–1278.
[47] F. Petit, M. Chalon, W. Friedl, M. Grebenstein, A. Albu-Schäffer, G. Hirzinger, Bidirectional antagonistic variable stiffness actuation: Analysis, design & implementation, in: 2010 IEEE International Conference on Robotics and Automation, IEEE, 2010, pp. 4189–4196.
[48] N.G. Tsagarakis, I. Sardellitti, D.G. Caldwell, A new variable stiffness actuator (compact-vsa): Design and modelling, in: 2011 IEEE/RSJ International Conference on Intelligent Robots and Systems, IEEE, 2011, pp. 378–383.
[49] S.S. Groothuis, G. Rusticelli, A. Zucchelli, S. Stramigioli, R. Carloni, The variable stiffness actuator vsaut-II: Mechanical design, modeling, and identification, IEEE/ASME Trans. Mechatronics 19 (2) (2013) 589–597.
[50] A. Schepelmann, K.A. Geberth, H. Geyer, Compact nonlinear springs with user defined torque-deflection profiles using cam mechanism for variable stiffness actuators, in: 2014 Ieee International Conference on Robotics and Automation (Icra), IEEE, 2014, pp. 3411–3416.
[51] G.E. Forsythe, W.R. Wasow, Finite difference methods, Partial Differential (1960).
[52] B.S. Mordukhovich, Sensitivity analysis in nonsmooth optimization, Theor. Aspects Ind. Des. 58 (1992) 32–46.
[53] S. Boyd, L. Vandenberghe, Convex Optimization, Cambridge University Press, 2004.
[54] J.-P. Vert, Nonlinear optimization: Duality, 2006.
[55] G. Pillo, M. Roma, Large-Scale Nonlinear Optimization, Vol. 83, Springer Science & Business Media, 2006.
[56] C.-L. Chang, R.C.-T. Lee, Symbolic Logic and Mechanical Theorem Proving, Academic Press, 2014.
[57] M.H. Karwan, R.L. Rardin, Surrogate duality in a branch-and-bound procedure, Nav. Res. Logist. Q. 28 (1) (1981) 93–101.
[58] M. Dawande, J.N. Hooker, Inference-based sensitivity analysis for mixed integer programming, Oper. Res. 48 (4) (2000) 623–634.
[59] J. Skorin-Kapov, F. Granot, Non-linear integer programming: sensitivity analysis for branch and bound, Oper. Res. Lett. 6 (6) (1987) 269–274.
[60] R.E. Moore, R.B. Kearfott, M.J. Cloud, Introduction to Interval Analysis, Vol. 110, Siam, 2009.
[61] S. Sakai, S. Stramigioli, Visualization of hydraulic cylinder dynamics by a structure preserving nondimensionalization, IEEE/ASME Trans. Mechatronics 23 (5) (2018) 2196–2206.
[62] M. Solimanpur, A. Jafari, Optimal solution for the two-dimensional facility layout problem using a branch-and-bound algorithm, Comput. Ind. Eng. 55 (3) (2008) 606–619.
[63] H. Ratschek, J. Rokne, New Computer Methods for Global Optimization, Horwood Chichester, 1988.
[64] M.G. Catalano, G. Grioli, F. Bonomo, R. Schiavi, A. Bicchi, Vsa-hd: From the enumeration analysis to the prototypical implementation, in: 2010 IEEE/RSJ International Conference on Intelligent Robots and Systems, IEEE, 2010, pp. 3676–3681.
[65] M.G. Catalano, G. Grioli, M. Garabini, F. Bonomo, M. Mancini, N. Tsagarakis, A. Bicchi, Vsa-cubebot: A modular variable stiffness platform for multiple degrees of freedom robots, in: 2011 IEEE International Conference on Robotics and Automation, IEEE, 2011, pp. 5090–5095.
[66] W. Friedl, M. Chalon, J. Reinecke, M. Grebenstein, et al., Fas a flexible antagonistic spring element for a high performance over, in: 2011 IEEE/RSJ International Conference on Intelligent Robots and Systems, IEEE, 2011, pp. 1366–1372.